Intramolecular Path Determination of Active Electrons on Push-Pull Oligocarbazole Dyes-Sensitized Solar Cells

Salma Trabelsi,[a] Nouha Kouki,[a] Mahamadou Seydou,[b] François Maurel,[b] and Bahoueddine Tangour*[a]

Several push-pull oligocarbazole dye-sensitizers have been studied using theoretical methods in order to better understand the relationship between structural electronic or optical properties and intramolecular path of active electrons during the ionization and injection processes. DFT/TD-DFT calculations were performed on a series of five dye sensitizers. They differ by the presence of electron donating group (EDG) by inductive effect (noted +I) or electron releasing group (ERG) by mesomeric effect (noted +M) or electron withdrawing group by inductive effect (noted-I) on the pushed part of the dyes studied. Our work focused on the internal distribution of electrons in the different parts of dye that are the push/pull moieties and the π-bridge. The study concerned the ground state, the electronic transition process and the excited state. In each situation, the fragment acting in the ionization or transition phenomena were identified. In the ground state, the electrons of the push part appear to be the least bound because they have the highest probabilities of ionization. In the excited state, the ionized atoms are essentially positioned in the pushing part and some neighboring atoms of the bridge. In the electronic transition, the active atoms are located in the π-conjugated part but only on the side adjacent to the acceptor group. To arrive to this conclusion, we optimized the structures of the five dyes in their ground and excited states. We calculated the atomic charges, the wavelengths and intensities of electronic transitions in the visible domain, the reorganization energies as well as the oxidation potential. It appears that +M donor ligands improve the performance of a dye because the great distribution of atoms to be ionized in the push parts.

Introduction

Dye sensitized solar cells (DSSC) as a new type of photovoltaic devices were given full attention since the first work of O'Regan and Gratzel in 1991.[1–4] Their principle advantages are a good efficiency and a lower cost compared with conventional photovoltaic devices based on inorganic semiconductors and silicon. DSSCs are composed of dye sensitizers anchored on nanocrystalline titanium dioxide (TiO$_2$) deposited on a transparent conductive oxide glass, against platinum electrode and redox electrolyte. So far, the most energy DSSC conversion efficiency of 12.3% has been reported.[5] More recently, perovskite photovoltaic devices have been developed and led to 22% efficiency[6] but they present a great problem of stability which further limits their use.[7] Thus, different dyes have been studied. Although ruthenium-based chromophores such as N3/N719 and black dyes have been commonly used as dye sensitizers, the higher cost and the environmental problems prevent them from large-scale application.[8–12] Another class of dyes has been developed characterized by organic dyes that have a push-pull configuration, based on a dipolar electron donor D, π-bridge spacer and electron acceptor A (D-π-A) system, the acceptor ligand being anchored to the semiconductor surface. This structure can induce the transfer of intramolecular charge from the donor unit to the acceptor moiety through the π-bridge spacer and then promotes the excited electrons of the dyes to be injected into the conduction band of the semiconductor. To obtain highly effective DSSC devices, the dye sensitizers must meet the following requirements:[13] (i) strong adsorption between the dye acceptor and the semiconductor substrate to provide stable charge transfer channels and rapid electron injection, (ii) a driving force large enough to generate effective electrons from the excited dye sensitizers to the semiconductor conduction band, (iii) a large and strong absorption spectrum through visible and near infrared light to ensure efficient charge separation and increases the overall efficiency of solar conversion, (iv) a higher oxidation potential of the dye in the fundamental state than the redox couple (generally I$^-$/I$_3^-$) in order to ensure rapid regeneration of the oxidized dyes, (v) a sufficiently stable photo-thermal configuration to ensure that the DSSC device can operate much longer time. Our study will focus on the in-depth study from the chemist's point of view.

Heretofore, the best-performing DSSC is (SM 315) which is based on an organometallic porphyrin dye of the donor-bridge-acceptor type and has been reported by Grätzel et al.[14] that have certified recorded efficiencies of about 13% measured in direct sunlight and on laboratory scale equipment.

[a] S. Trabelsi, N. Kouki, B. Tangour
University of Tunis El Manar, Research Unity of Modeling in Fundamental Sciences and Didactics, IPEIEM, BP 254, El Manar 2, 2096 Tunis, Tunisia
E-mail: bahoueddine.tangour@ipeiem.utm.tn
[b] M. Seydou, F. Maurel
University Paris Diderot, Sorbonne Paris Cite, ITODYS. UMR 7086 CNRS, 15 rue J. A. de Baïf, 75205 Paris Cedex 13, France.
An invited contribution to a Special Collection dedicated to Computational Chemistry

However, metal-free organic dyes have recently received more attention than metal organic dye complexes.[15] This is due to their low toxicity, high molar extinction coefficient, easy accessibility, lightness, cost-effectiveness and facile fabrication.

The carbazole-based solar cells form an important class subject to sustained research[16–19] because their strong electron-donating ability and easy structural modification. They exhibit good light-harvesting a relatively high efficiency of up to 7.13%.[20–22]

Among Important factors that influence the performance of DSSC we can note:

(i) light recovery properties of dyes, (ii) aligning the lowest unoccupied molecular orbital (LUMO) near the anchor group and above the edge of the TiO2 conduction band, (iii) adjust the energy levels by introducing π-bridge units, and (iv) the properties of the redox couple in the electrolyte.

Carbazole unit in a DSSC may play role as donor, auxiliary donor and π-linker. So, understanding structure-ownership relationships is crucial for building efficient DSSC devices. In this paper, we will be interested on the electronic distribution in molecules and ions involved in the processes of excitation and ionization of push-pull dyes. This also includes intramolecular transfers during those processes.

In the context of the development of dyes for DSSCs, the electron acceptor part (A) is always located on the carboxylic acid grafting function, which has an electro-attracting character. Because of the presence of the π-conjugated spacer, the electron donor part is spatially spaced from the surface of the semiconductor. These two parts, donor and electron acceptor, are finally bridged by a poly aromatic π-conjugated system containing a bis-thiophenyl unit and an additional phenyl or naphthyl group. The electron donating part of the studied chromophores is thus based on the carbazole motif, which ensures good light absorption properties, but also guarantees an energy level of the ground state of the molecules suitable for the use of electrolytes with high oxidation potential[23–25] at the other end of the dyes. The cyanoacrilic acid group acts as both an electron acceptor and an attachment group.[26]

To analyze each phenomenon separately, simplified dyes SD1-5 shown in Figure 1 have been chosen. Two strategies have been developed by several modifications acted on SD1 considered as reference model: firstly, the addition of multiple visible-light-absorbing motifs and secondly, the introduction of a group richer in electron in the π-conjugated bridge. The former one consists on combining several carbazole units into the same molecule (SD1, SD2 and SD3).[27–30] The carbazole units have been substituted either by tert-butyl chain tBu (SD2) or by methoxy group OCH$_3$ (SD3) in order to highlight donor groups +M/+I or acceptor ones −I effects. The latter way focuses on the introduction of a naphthyl unit in place of the phenyl ring of the conjugated π-spacer (SD4 and SD5 chromophores). The only difference between these two dyes is the push part. The SD4 chromophore has a single carbazole unit, while the SD5 dye has three carbazole units. This dye differs from SD2 in the presence of naphthyl instead of phenyl. Indeed, the naphthyl unit is known to favor the transfer of intramolecular charge[31]

and has in particular made it possible to obtain an improvement in the molar extinction coefficient for similar sensitizers.[32]

Accordingly, we investigate the influence of novel organic D—π—A dyes SD1-5 containing various donor moieties based on the carbazole motif on the performance of DSSC according to their geometries, electronic structures of ground and first excited state energy levels, and absorption properties. The purpose of this study is to determine by calculation the intrinsic properties of the dyes and explain the elementary processes involved in these devices.[3] It is trivial to indicate that the properties of similar organic compounds are well investigated for decades now. However, our main challenge is to analyze, from the chemist's point of view, the electron distribution on each atom to clarify its role during the excitation and ionization processes. This would allow certain atoms to be declared as the main portals for efficient electron injection of the dye to TiO$_2$. This will open horizons for further study of this injection process which is underway in our laboratory.

Computational Details

All molecular calculations were performed in the gas phase, in dichloromethane and in methanol solutions using the density functional theory (DFT) method implanted in the Gaussian (09) program package.[33] The geometry optimization of all the dyes on the electronic ground state have been performed at the DFT level,[34,35] with the hybrid B3LYP exchange correlation functional[36,37] and the 6-311G (d) basis set.[38] This method has been proved to be a precise formalism to calculate the characteristic parameters of many dyes.[39] To determine the excitation energies using the adiabatic approximation, we performed an approach adapted to the time-dependent density functional theory (TD-DFT)[40,41] with B3LYP,[42] CAM-B3LYP[28] hybrid functional to calculate the vertical excitation energy of dyes.

The previous theoretical studies confirm that the solvent effect is related to describe the absorption spectra of the dyes. The result of calculation using the CAM-B3LYP functional is in good agreement with the experimental value. Therefore, we adopted the TD-CAM-B3LYP functional with the 6-311G (d) basis set, combining the conductor-like polarizable continuum model (CPCM) in dichloromethane and in methanol solutions for predicting optical properties of dyes. Subsequently, the obtained data were analyzed using the SWizard program.[43] In addition, in order to evaluate the ionization potential (IP) and the electronic affinity (EA), all the dyes in cationic and anionic states are fully optimized on the ground state. The oxidation potential of all the isolated molecules from the ground state was reached with the level C-PCM[44] B3LYP/6-311G (d) by calculating single points in their neutral and cationic states to evaluate the free Gibbs energy change for electron injection from an excited state of dyes to the TiO$_2$ conduction band. The Natural Binding Orbital (NBO) analysis[45] was performed at the B3LYP/6-311 G (d) level and at the C-PCM TD-CAM-B3LYP/6-311 G (d) level for all the atoms. To gain more comprehension in this work, we explored the reorganization energies of both

holes and electrons to better describe the transport phenomenon and the charge transfer process of these different sensitizers.

Results and Discussion

3.1 Ground State

3.1.1 Conformation Study

This part concerns both the organic molecules and their cationic especies resulting from the ionization process. The goal is multiple. The comparison of optimized geometry and experimental structures is often used as a means of validating the adopted calculation level. The comparison of the bond length changes of the molecules and their cations provides information on the local zones contributing to ionization such as chemical bonds or lone pairs

Structure of dyes has an essential role on the performance of the DSSC because the direct relation between geometrical modifications induced by ionization process and hole mobility. This later property may be sensitive to any change in dye structure or to the nature of ligands. Thus, the effect of changing the donor group and the π-conjugated bridge were discussed in detail in this study for the five investigated dyes. The optimized ground state geometry of SD1-5 has been reported in Figure 1 and selected torsion angles are listed in Table 1. From the optimization of different geometries, it is clear that the theoretical values are very close to experimental ones which validate the adopted calculation method.

We observed that the structures are almost flat. The inclination angle (Θ_2 and Θ_3) between the external and the carbazole central units are shown in Table 2. Their values range
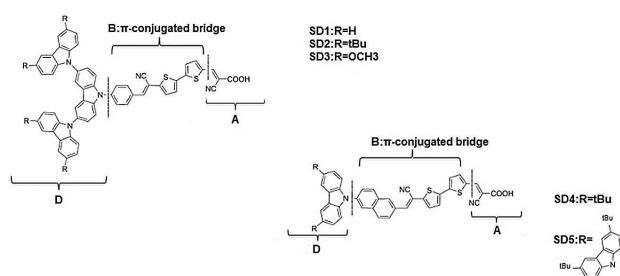
Table 2. Inter- ring angle in degrees (°), Dipole moment in Debye (D), Ionization potential and Electron affinity (eV) computed for relaxed SD1-5 at the ground state. For convenience, Dipole moment values of the first excited state are integrated in this Table.

| | Inter-ring angle (°) | | | Dipole moments μ (D) | | IP | EA |
	Θ_1	Θ_2	Θ_3	Ground state	Excited state		
SD1	53.8	63.3	62.5	3.11	3.84	6.37	2.59
SD2	52.8	60.1	59.9	2.93	3.53	6.18	2.59
SD3	53.3	58.9	59.4	3.87	4.25	6.01	2.36
SD4	50.8	–	–	4.95	4.95	6.48	2.45
SD5	55.3	60.8	61.9	3.17	3.79	6.15	2.59

from 58° to 63°, which agrees with the experimental ones (54° to 76°).[26] On the other hand, the angle (Θ_1) defined by the central carbazole and the phenyl or naphthyl is between 50° and 55°, which is close to the experimental data (46°–57°).[26] All those angle values are less than 90°.

This allows an extensive delocalization of electronic density from the donor portion to the acceptor part passing by the spacer portion. To understand the origins of the electron transfer mechanism in the dyes, we performed the natural bond orbital (NBO) analysis. This study was carried out on the basis set used for the optimized geometry in the ground state and in the excited state in the CH_2Cl_2 solution (Table 3). We summed

Table 3. NBO atomic charge of the ground state (S_0) and excited state (S_1) of the five dyes SD1-5. The push, π-conjugated and pull parts are designed by D, B and A respectively. $\Delta q(D)$ represents the difference in electronic charge between the excited and ground states of a dye.

| Dyes | Ground state | | | Excited state | | | $\Delta q(D)$ |
	D	B	A	D	B	A	
SD1	0.16	−0.04	−0.12	0.19	−0.04	−0.15	0.03
SD2	0.16	−0.02	−0.14	0.19	−0.04	−0.15	0.03
SD3	0.16	−0.02	−0.14	0.19	−0.04	−0.15	0.03
SD4	0.18	−0.03	−0.15	0.20	−0.05	−0.15	0.02
SD5	0.16	−0.02	−0.14	0.19	−0.04	−0.15	0.03

Figure 1. Molecular structures of the five studied dyes SD1-5

Table 1. Selected bond lengths in Å of the studied dye SD1.

Bond length	Theo	Exp.[26]
N94–C54	1.423	1.423
N95–C51	1.423	1.423
N57–C36	1.415	1.416
C29–C25	1.453	1.454
C24–C22	1.461	1.460
C17–C15	1.440	1.439
C10–C1	1.428	1.425
C1–C2	1.365	1.366
C2–C6	1.483	1.483

charges of all atoms belonging to one part (A, D or B) of each dye. According to the values gathered in Table 3, we notice that all electron donating parts of dyes have positive charges. This shows that these units have the ability to eject electrons. In contrast, the π-conjugated and the accepting groups have the negative charges. In this case, it can be concluded that these parties have the ability to trap electron. The relatively poor polarity of the bridge part indicates that its π system plays its role assigned to transmitter the "electronic information" from A to the D parts of the dye.

One of the most important elements to evaluate is the conjugation length of the π electron system. NBO analysis is considered as one of the powerful tools to access à this information. We calculated Wiberg bond indices WBI (Table 4). We note a decrease by roughly 0.2 of multiple bond WBIs (C4≡N5 and C6≡O7) and by contrast an increase by the same quantity of single bond WBIs of (C1–C10, C15–C17). This testifies of the great conjugation being in the A part of those dynes. Similar behavior is detected in the bridge group. Indeed,

Table 4. Wiberg Bond Indices (WBI) in molecular (M) and univalent cationic (M$^+$) states.

Part		SD1 M	SD1 M$^+$	SD2 M	SD2 M$^+$	SD3 M	SD3 M$^+$	SD4 M	SD4 M$^+$	SD5 M	SD5 M$^+$
A	C1-C10	1.19	1.20	1.22	1.20	1.22	1.21	1.22	1.20	1.22	1.21
	C4-N5	2.84	2.83	2.83	2.83	2.83	2.84	2.83	2.83	2.83	2.83
	C6-O7	1.76	1.75	1.74	1.75	1.74	1.75	1.74	1.76	1.74	1.75
	C6-O8	0.98	1.02	1.01	1.02	1.01	1.02	1.01	1.03	1.01	1.02
	C15-C17	1.15	1.17	1.16	1.16	1.16	1.16	1.16	1.20	1.16	1.17
B	C24-C25	1.68	1.57	1.59	1.58	1.59	1.59	1.58	1.50	1.59	1.58
	C25-C29	1.08	1.16	1.15	1.15	1.15	1.14	1.15	1.21	1.15	1.15
	C27-N28	2.86	2.85	2.85	2.85	2.85	2.85	2.84	2.85	2.85	2.85
D	C36-N57	0.99	0.98	0.99	0.97	0.99	0.96	0.99	1.04	0.96	1.01
	C51-N95	0.97	1.01	0.97	1.01	0.97	0.99	–	–	0.96	1.01
	C54-N94	0.97	1.01	0.966	1.01	0.97	0.92	–	–	0.97	1.01

WBI of double and triple bonds decrease strongly. But any signifying change in bond orders of the D part was observed. Our results highlight the great conjugation length that includes actually the totality of the A and the bridge B parts.

The dipole moment of the pigment plays an important role both in the electron spectrum and in the injection process. In Table 2, we gathered also the values of the dipole moments μ of all the studied dyes in the ground and excited states. We observed that the dipole moment values are sensitive to the substituent nature. By comparing those of dyes SD1, SD2 and SD3 in their ground state, we see that dipole moment increases from 3.84 D for the unsubstituted SD1 to 4.25 D for the SD3 bearing the polar methoxy group. The presence of a +I donating group tBu does the dipole moment of SD3 decrease to the value of 2.93D.

Characteristic parameters such as ionization potential (IP) and electronic affinities (EA) are also important factors in the rational design of photovoltaic cells, in particular the charge mobility. So, adiabatic IP and EA are calculated from neutral, cationic and anionic states of the optimized dyes (Table 2). We can consider that those quantities, because they are a difference of energies, are just a little depending of the modifications introduced in SD2-4 relatively to SD1.

3.1.2 Ionization Probability in the Ground State (IPr)

In some cases, the analysis of geometrical modifications induced by ionization process is able to indicate such as gates if there are great changes in bond orders. Comparison of Wiberg indices of molecules and cations listed in Table 4 does not us to detect any signifying differences. This is an indication that in both entities there is an important delocalization that attenuates expected changes. We introduced another way to detect and hierarchize such exit gates using their ionization probability. In this section we will rank the atoms of each dye in terms of the probability of ionization. This part of our paper represents the principal challenge of our study and a new approach in analyzing ionization process of organic dyes. We define the probability of ionization by the electron population variation Δq (M, M$^+$) of each atom of the molecule M and the corresponding cation M$^+$ expressed as a percentage.

As this calculation only concerns atom whose variation Δq (M, M$^+$) is positive and greater than an arbitrarily fixed threshold, we proceed to a normalization operation to obtain the ionization probabilities. The choice of this threshold is established when we observe a significant difference. The obtained values have no significance in themselves but serve to highlight all the atoms most likely to be ionized. This operation was done for the molecules and their cations at the both in the ground state and in the excited state through TD-DFT calculations.

The ionization probability (IPr) of each atom will allow us to locate the "exit gates" of the electrons and to compare the dye's ability to electron injection in the semiconductor oxide. To calculate the ionization probability values, we used the following equation:

$$IPr(\%) = \frac{\Delta q_{NBO} \text{ of the atom}}{\sum \Delta q_{NBO}} * 100$$

In Figure 2, we showed the most ionized sites in the five dyes. They have the highest ionization probability values. In Table 5, we have gathered the most important ionization probability values of the atoms in the five studied dyes SD1-5.

In the dyes SD1 and SD4, it can be seen that the ionized sites are distributed on the different parts of the molecule. On the other hand, in the case of SD2, SD3 and SD5, the sites are concentrated on the push part of dyes. This is due to the substitution on carbazole units by electron donor effects,
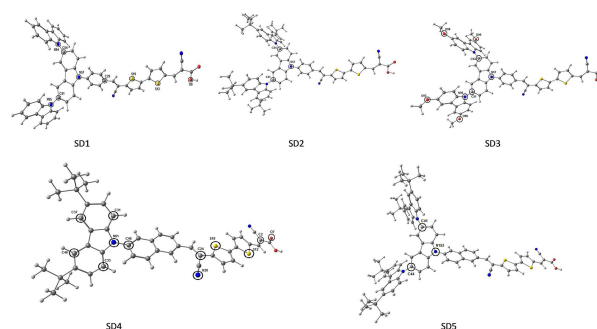
Figure 2. The ionized sites in the ground state for the five studied dyes SD1-5.

Table 5. The principal ionization probabilities IPr of the atoms in each studied dye.

SD1 Atom	IPr	Z	SD2 Atom	IPr	Z	SD3 Atom	IPr	Z	SD4 Atom	IPr	Z	SD5 Atom	IPr	Z
C 29	20.88	D	C 54	41.90	D	C 54	16.4	D	S 12	12.56	B	C 41	43.08	D
N 57	15.18	D	C 51	20.59	D	C 51	15.52	D	S 19	11.88	B	C 44	40.24	D
N 95	10.72	D	N 57	9.41	D	O 96	12.38	D	C 45	11.40	D	N 153	16.68	D
N 94	10.42	D				O 99	12.05	D	N 61	9.10	D			
S 19	9.69	B				O 97	11.53	D	C 24	7.86	B			
C 54	8.85	D				O 98	11.32	D	C 33	7.74	D			
S 12	8.65	B				N 57	10.78	D	O 7	7.10	A			
O 8	8.37	A				N 95	10.01	D	C 31	6.74	D			
C 51	7.25	D							N 28	6.62	B			
									C 37	6.46	D			
									C 40	6.32	D			
									C 2	6.20	A			

inductive (+I) in the case of SD2 and SD5 or mesomeric (+M) in the case of SD3.

3.1.3 Frontier Molecular Orbitals

The nature of the frontier molecular orbital of these dyes in the ground state is explored by DFT calculations. The results show that there is a good spatial separation of the frontier molecular orbital in all cases, as illustrated in Figure 3. A good correlation between the two theoretical calculations is observed by comparing the results obtained by a DFT/B3LYP/6-311G (d) calculation and another work done at DFT/B3LYP/6-31G(d).[26]

By analyzing the frontier molecular orbitals of the five dyes, we find in the case of SD1-3, the HOMO is located on the three carbazole units with a low contribution to the π-conjugate spacer. But, in the case of SD4, the HOMO is delocalized on the naphthyl unit and part of the π-conjugated bridge. The LUMO of the dyes is centered on the accepting part of the molecule with a large contribution of its orbitals. We also observe a strong delocalization on the π-conjugate spacer.

This spatial distribution of the frontier orbitals, observed for all the dyes, favors the separation intramolecular of the charge and improves the efficiency of electron injection from the excited state of the dye into the semiconductor oxide, which limits the phenomena of recombination.

The energy of the atomic orbital composition of the highest- occupied and lowest unoccupied molecular orbital (HOMO and LUMO) of SD1-5 push- pull dyes are shown in Table 6. It is noted that the values found by the theoretical calculation are in approach with the values found experimentally. The optical gaps (ΔE) thus determined are between 1.62 eV and 2.25 eV for the whole series calculated at the DFT/ B3LYP/6-311G (d) level.

Moreover, the methoxy groups grafted into the carbazole unit of the electron donor part are responsible for the destabilization of the levels HOMO and LUMO and, consequently, reduction of the gap (Eg) to reach 1.67 eV in the case of SD3. In addition, we note a slight destabilization of the HOMO and LUMO energy levels of SD5 dye relative to the SD2 dye. This situation is explained by the replacement of a naphthyl unit instead of the phenyl ring the π-conjugate bridge. The additional electron donor group's effect on HOMO
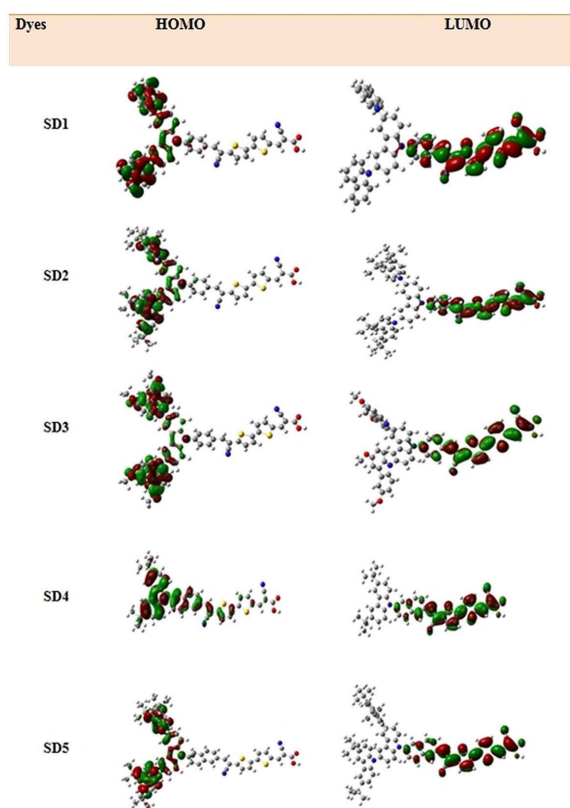

Figure 3. Frontier orbitals of the oligocarbazole dyes SD1-5 plotted with an isovalue of 0.02 using DFT/B3LYP/6-311G (d) method.

Table 6. HOMO, LUMO and band gap energy values of different studied dyes.

Dyes	E_{LUMO} (eV)	E_{HOMO} (eV)	gap energy Theo.
SD1	−3.48	−5.56	2.08
SD2	−3.45	−5.39	1.94
SD3	−3.44	−5.06	1.62
SD4	−3.35	−5.60	2.25
SD5	−3.46	−5.37	1.91

and LUMO levels was also discussed. The LUMO level must be sufficiently negative with respect to the conduction band of TiO$_2$ to inject electrons effectively and the HOMO level should be more positive than the redox potential of I$^-$/I$_3^-$ for efficient dye regeneration. To estimate the possibility of electron injection to the conduction band of the TiO$_2$ and electron regeneration from the redox couple, the HOMO and LUMO energy levels of the five dyes were calculated. The energy diagram is shown in Figure 4a.
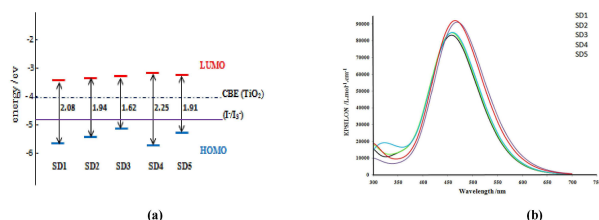
Figure 4. a) Schematic energy diagram for the five studied dyes SD1-5, the conduction band (CBE) of the anatase TiO$_2$ surface (-4.0 eV) and I$^-$/I$_3^-$ redox electrolyte (-4.8 eV). **b)** The calculated spectra for the oligocarbazole based dyes dissolved in dichloromethane at CPCM/TD-DFT/CAM-B3LYP/6-311G (d) level of theory

As shown, the HOMO levels of oligocarbazole based dyes were systematically decreased when adding more donor ability approaching the redox potential of the electrolyte system. Compared with the electrolyte redox potential, these HOMO levels were below the iodine/iodide redox potential. These results show the ability of dyes to accept electrons generated from the redox couple .For LUMO levels, the results show that the change of substituent on the carbazole motif and the replacement of phenyl by naphthyl unit slightly affected the LUMO level. However, the LUMO levels of all the dyes were above the TiO$_2$ conduction band. This shows a good electron injection into the conduction band (CB) of TiO$_2$ semiconductor.

3.2 Excited States Studies

3.2.1 UV-Visible Spectrum

The simulated electronic absorption spectra of all dyes in dichloromethane and methanol solvents at CPCM-TDCAM-B3LYP/6-311G (d) level of the theory is shown in Figure 4b. All dyes exhibit intense absorption in the visible range, centered between 458 and 465 nm. A good correlation between the theoretical and experimental values is observed.[26] A broad absorption band extending from 400 nm to 550 nm is observed in all cases.

Such behavior makes it possible to envisage a relatively high photo-generation of charges for the solar cells sensitized with these dyes. The high molar absorption coefficients are comparable to those obtained for organic chromophores (i.e. C212[46]) and even higher than those obtained for other chromophores of the carbazole type (i.e. TC306[24]), which validates the approach developed in the case of SD1-5 dyes.

During the excitation, the electrons on the dye-donor carbazole group are transferred to the π-conjugated moiety and then migrate to the cyanoacrylic acid moiety. This is consistent with the role of the π- conjugated spacer.

That is, the electrons could be transferred from the donor group to the π-conjugated spacer, then transferred to the acceptor/anchoring group and finally injected into the TiO$_2$ semiconductor. As seen from Table 3, the charge differences on donor group between S$_1$ and S$_0$ in all dyes indicate that the dyes SD1-3 could donate more electrons as compared to SD4 and SD5.

It clearly shows that their construction helps to delocalize electron on the entire dye and with less overlap between the donor group and the acceptor/anchoring group, therefore, reduce the loss of electron.[47] From Figure 5, we noted that the HOMO is delocalized on the naphthyl unit and part of the π-conjugated bridge. Conversely, the LUMO of the dyes is systematically centered on the opposite part of the molecule, the cyanoacrylic group. This distribution of HOMO and LUMO is separated in the compound, which indicates that the transition HOMO→LUMO can be considered as an intramolecular transfer of charge (ICT) transition.

When the sensitizer dye is anchored to TiO$_2$, the position of the LUMO close to the anchor group improves the orbital overlap with the titanium 3d orbital and promotes the injection of electrons. On the other hand, HOMO-2 and LUMO are located on the same fragment, indicating that the transition HOMO-2→LUMO can be considered as a transition π-π*. In addition, the distribution of HOMO-1 and LUMO is separated in the compound, which indicates that the transition HOMO-1→LUMO can be considered also as an intramolecular transfer of charge (ICT) transition.
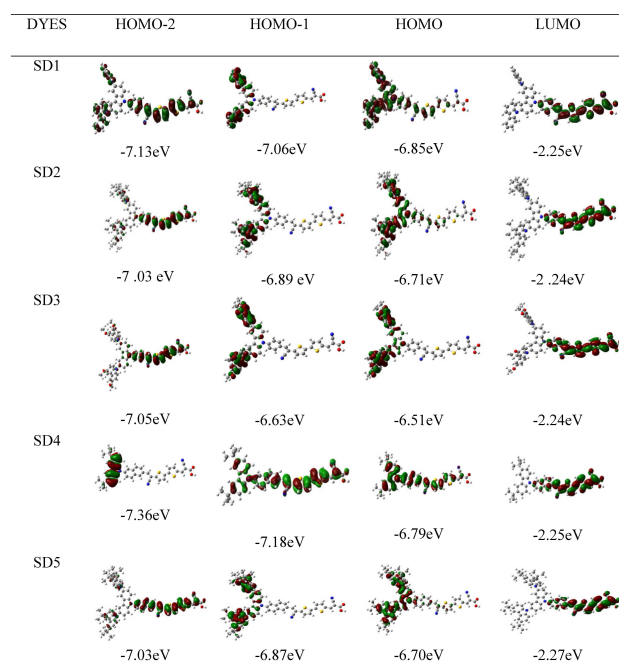
Figure 5. Selected frontier molecular orbitals of all dyes: (HOMO-2, HOMO-1, HOMO and LUMO) calculated from TD-DFT using the CAM-B3LYP functional.

Table 7. Electronic transition data obtained by TD-DFT/CAM-B3LYP/6-311G (d) level for SD1-4 dyes in the CH_2Cl_2 solution and SD5 in the methanol: wavelength λ(nm). Energy ΔE (eV) and oscillator strength f. H-2, H-1, H and L represent HOMO-2, HOMO-1, HOMO and LUMO respectively.

Dyes	Parameters				Transition	
	λ_{exp}	λ_{theo}	ΔE	f	Origin	character
SD1	462	458	2.71	2.05	H-2→L(+62%)	π→π* (B→B)
					H →L(+26%)	ICT (D→A)
SD2	465	458	2.70	2.08	H-2→L(+72%)	π→π* (B→B)
SD3	465	460	2.70	2.09	H-2→L(+78%)	π→π* (B→B)
SD4	470	469	2.64	2.24	H →L(+49%)	ICT (D→A)
					H-1→L(+40%)	π→π* (B→B)
SD5	454	465	2.67	2.26	H-2→L(+75%)	π→π* (B→B)

Figure 6. The ionized sites in the excited state for the five dyes.

In Table 7, we report experimental and computed absorption maximum, oscillator strengths and composition in terms of molecular orbital contributions for the five energy electronic transitions. The absorption spectrum and the frontier orbital show that the main transition corresponds to the transition π→π* associated with the HOMO-2→LUMO configuration for the chromophores SD1, SD2, SD3 and SD5. Compared to SD4, the transition HOMO→LUMO can be considered an intramolecular transfer of charge (ICT).
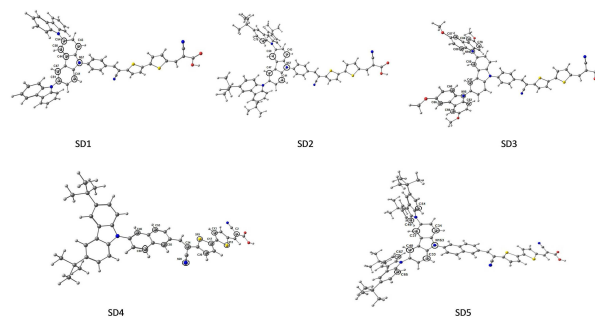
This analysis allowed us to locate the zone responsible for the electronic transition detected in the visible. Except in SD4 the nature of transition is a charge transfer against the others are of nature π-π*.

3.2.2 Ionization Probability in the Excited State (IPr*)

We studied also the Ionization Probability in the excited state (IPr*) as defined in the paragraph below. In Table 8, we have gathered the most important ionization probability values of the atoms in the five dyes. The most important sites are indicated in Figure 6. Except for SD4, the ionized atoms are close to the pull part. For SD4, it's the opposite; the atoms of the push part are the least bound. For the dyes SD1, SD2 and SD5, the ionized atoms are located in the pushing part. This highlights the important role substituted on the carbazole unit.

In the dye SD3, the ionized sites are placed on the two carbazole units which are substituted by methoxy groups.

From values gathered in Table 3, we can see that the excited state is more polarized than the ground state because the charge variation of the D part Δq (D) is about 0.03 electrons. This information confirms the hypothesis of efficient electron injection from the excited state M*.

3.3 Global Properties

We will deal in this paragraph with two global properties of DSSCs that are the reorganization energy and the oxidation potential. The former, the intramolecular reorganization energy, is the energy cost of geometry modifications to go from a neutral M* to a charged oligomer M^+ in the process of photo ionization. It is one of the key characteristics that control charge mobility in organic electronics.

Reorganization energy, even for a hole or an electron, can be stated with the Marcus equation:[48–51]

$$K = \frac{4\pi 2}{h} \frac{1}{\sqrt{4\pi\lambda k_B T}} V^2 \exp\left(-\frac{\lambda}{4\pi k_B T}\right) \tag{1}$$

h: Planck constant
k_B: Boltzmann constants
T: Temperature

Table 8. Ionization Probability (IPr*) values of atoms in the excited state of the five studied dyes. The zone Z of the "push", π-conjugated bridge and "pull" parts.

SD1 Atom	IPr*	Z	SD2 Atom	IPr*	Z	SD3 Atom	IPr*	Z	SD4 Atom	IPr*	Z	SD5 Atom	IPr*	Z
N 57	17.40	D	C 43	18.53	D	C 87	9.56	D	S 19	13.45	B	C 31	15	D
C 41	17.40	D	C 41	18.35	D	C 66	9.46	D	C 55	11.80	D	C 33	15	D
C 43	16.58	D	C 50	17.91	D	C 84	8.94	D	C 24	10.27	B	C 37	14	D
C 47	14.29	D	C 47	17.85	D	C 69	8.87	D	C 17	9.58	B	C 40	14	D
C 50	12.78	D	N 57	15.79	D	C 80	8.21	D	C 20	8.98	B	N153	13	D
C 51	7.86	D	C 78	11.57	D	C 60	8.10	D	S 12	8.85	B	C 49	8	D
C 54	7.01	D				C 78	8.10	D	C 50	6.60	A	C 51	8	D
C 44	6.69	D				C 62	8.05	D	C 46	6.51	A	C 65	7	D
						N 94	7.94	D	C 53	6.26	A	C 67	7	D
						N 95	7.87	D	C 13	6.04	B			
						C 47	7.51	D	N 28	5.93	B			
						C 50	7.39	D	C 2	5.75	B			

Table 9. Experimental and calculated photovoltaic characteristics of dyes SD1-5 in DSSC using a I^-/I_3^- electrolyte type and a TiO_2 film thickness of 15 μm.

Dyes	Experimental values[26]					Theoretical caculations						
	J_{SC}	V_{OC}	FF	η(%)	E_{ox}	λ_1	λ_2	λ_3	λ_4	λ_{hole}	$\lambda_{electron}$	E_{ox}
SD1	11.68	0.58	72	4.9	1.43	0.07	0.08	0.18	0.18	0.15	0.36	1.63
SD2	13.45	0.59	72	5.8	1.22	0.07	0.07	0.19	0.18	0.13	0.37	1.56
SD3	14.33	0.56	72	5.8	1.06	0.08	0.08	0.19	0.18	0.16	0.37	1.50
SD4	13.83	0.58	69	5.6	1.37	0.06	0.06	0.16	0.16	0.13	0.32	1.55
SD5	11.76	0.62	74	5.4	1.30	0.07	0.07	0.16	0.16	0.14	0.32	1.55

λ: The reorganization energy for hole or electron.

V: The intermolecular electronic transfer integral between neighboring molecules.

The intermolecular hole and the electron transfer processes can be given by the following equation:

$$M^{+/-} + M^* \rightarrow M^* + M^{+/-} \qquad (2)$$

$M^{+/-}$ indicates the molecule M in a cationic or anionic state.

M^* is a neighboring molecule in the fundamental state.

In Figure 7, we have represented the potential energy curves. The reorganization energy of the holes transport λ_{hole} is given by $\lambda_1 + \lambda_2$. Similar one relatively to the electron is noted $\lambda_{electron}$ and calculated as the sum $\lambda_3 + \lambda_4$.
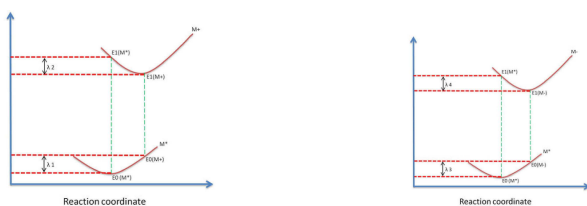
The transfer reorganization energy of the hole and the electron are defined by:

$$\lambda_{hole} = \lambda_1 + \lambda_2 = (E_0(M^+) - E_0(M^*)) + (E_1(M^*) - E_1(M^+))$$

$$\lambda_{electron} = \lambda_3 + \lambda_4 = (E_0(M^-) - E_0(M^*)) + (E_1(M^*) - E_1(M^-))$$

From values gathered in the Table 9, we can see that the values of λ_{hole} are smaller than those of $\lambda_{electron}$, which indicates better hole transport performance. If the SD1 and SD3 dyes are compared, we can observe a decrease in λ_{hole} and an increase in $\lambda_{electron}$.
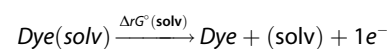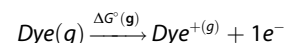
This is explained by the substitution of the hydrogen on the carbazole unit (in the case of SD1) by a methoxy group (in the case of SD3). Therefore, the transport process is determined by two important molecular parameters: the reorganization energy (λ), which must be small for efficient charge transport, and the integral of the intermolecular electron (V) or hole that describes the force electronic coupling between neighboring molecules.[52]

By comparing SD4 and SD5, there is a slight increase in hole reorganization energy. This is explained by the increase in the number of carbazole units in the electron donating moiety.

To find the oxidation potential, a method related to thermodynamics was used according to the following equation:

$$Dye(g) \xrightarrow{\Delta G^{\circ}(\mathbf{g})} Dye^{+(g)} + 1e^-$$

$$Dye(solv) \xrightarrow{\Delta rG^{\circ}(\mathbf{solv})} Dye + (solv) + 1e^-$$

Or:

$$\Delta G^{\circ}_{(\mathbf{solv})} = -\Delta G^{\circ}_{(\mathbf{solv})}(\mathbf{dye}) + \Delta G^{\circ}_{(\mathbf{g})} + \Delta G^{\circ}_{(\mathbf{solv})}(\mathbf{dye}^+)$$

It is also possible to calculate the oxidation potential E^0 (V) via equation:

$$E^0(V) = \frac{-\Delta G^{\circ}(solv)}{23.06}$$

The oxidation potentials E^0 were obtained in Table 9 by the solvation model CPCM on the Gaussian09 software in a solution of dichloromethane and methanol (since experimentally, the dyes SD1-4 are dissolved in dichloromethane and the dye SD5 in methanol during of the production of the DSSC). We noted that the oligocarbazole dyes had oxidation potentials greater than 1 V vs. NHE. This means that the HOMO level of these dyes is sufficiently higher than the redox potential of the electrolyte used in this study ($I^-/I_3^- + 0.4\ V^{[52]}$).

Conclusion

In this paper, we have presented a theoretical study of oligocarbazole based organic dyes for solar-cell devices. To gain a better understanding of the role of the sensitizer, particularly of its electronic structure and excited-state properties in the efficiency of DSSC devices, we performed DFT and TD-DFT calculations.

The good agreement between the experimental and TD-DFT calculated absorption spectra allowed us to provide a detailed assessment of the main spectral features of a series of dyes.

From the present study, we can note some general trends regarding the effect of the dependence of π-conjugation length and the influence of hydrogen substitution by electron donor groups such as (tBu and OCH_3). Increased conjugation length

Figure 7. Energy diagram of the inter-molecular transfer reaction between neutral molecule and cationic/anionic specie.

resulted in a more red-shifted spectral response in the case of SD4 and SD5.The dye with the methoxy group showed better absorbance efficiency than the dye with naphtyl unit and the two other dyes SD1-2, due to a larger dipole moment of the dye and the low gap energy. We have noticed that the SD3 dye has the good performance. In this case it will be a good candidate as dye sensitizer DSSC.

Conflict of interest

The authors declare no conflict of interest.

[1] M. Grätzel, *Nature* **2001**, *414*, 338–344.
[2] A. Hagfeldt, G. Boschloo, L. Sun, *Chem. Rev.* **2010**, *110*, 6595–6663.
[3] A. Hagfeldt, M. Grätzel, *Acc. Chem. Res.* **2000**, *33*, 269–277.
[4] B. O'Regan, M. Grätzel, *Nature* **1991**, *353*, 737–740.
[5] A. Yella, H-W. Lee, H. N. Tsao, *Science* **2011**, *334*, 629–634.
[6] W. S. Yang, B-W. Park, E. H. Jung, *Science* **2017**, *356*, 1376–1379.
[7] S. N. Habisreutinger, D. P. McMeekin, H. J. Snaith, *APL Materials* **2016**, *4*, 91503.
[8] W. Ghann, H. Kang, T. Sheikh, *Sci Rep.* **2017**, *7*, 41470.
[9] D. D. Pratiwi, F. Nurosyid, A. Supriyanto, *IOP Conf. Ser.: Mater. Sci. Eng.* **2017**, *176*, 12012.
[10] M. K. Nazeeruddin, P. Péchy, T. Renouard *J. Am. Chem. Soc.* **2001**, *123*, 1613–1624.
[11] M. K. Nazeeruddin, S. M. Zakeeruddin, R. Humphry-Baker, *Inorg. Chem.* **1999**, *38*, 6298–6305.
[12] M. K. Nazeeruddin, A. Kay, I. Rodicio, *J. Am. Chem. Soc.* **1993**, *115*, 6382–6390.
[13] D. P. Hagberg, J-H. Yum, H. Lee, *J. Am. Chem. Soc.* **2008**, *130*, 6259–6266.
[14] S. Mathew, A. Yella, P. Gao, R. Humphry-Baker, B. F. E. Curchod, N. Ashari-Astani, I. Tavernelli, U. Rothlisberger, M. K. Nazeeruddin, M. Grätzel, *Nat. Chem.* **2014**, *6*, 242–247.
[15] J. M. Juma, S. A. H. Vuai, N. S. Babu, *Int. J. Photoenergy.* **2019**, *2019*, 1–8.
[16] A. Venkateswararao, K. R. J. Thomas, C.-P. Lee, C.-T. Li, K.-C. Ho, *ACS Appl. Mater. Interfaces.* **2014**, *6*, 2528–2539.
[17] G. Sathiyan, E. K. T. Sivakumar, R. Ganesamoorthy, R. Thangamuthu, P. Sakthivel, *Tetrahedron Lett.* **2016**, *57*, 243–252.
[18] H. Jiang, J. Sun, J. Zhang, *Curr. Org. Chem.* **2012**, *16*, 2014–2025.
[19] R. Samae, P. Surawatanawong, U. Eiamprasert, S. Pramjit, L. Saengdee, P. Tangboriboonrat, S. Kiatisevi, *Eur. J. Org. Chem.* **2016**, *2016*, 3536–3549.
[20] H. Lai, J. Hong, P. Liu, C. Yuan, Y. Li, Q. Fang, *RSC Adv.* **2012**, *2*, 2427.
[21] K. R. Justin Thomas, A. Venkateswararao, C.-P. Lee, K.-C. Ho, *Dyes Pigm.* **2015**, *123*, 154–165.
[22] Z. Yang, C. Shao, D. Cao, *RSC Adv.* **2015**, *5*, 22892–22898.
[23] M. Cheng, X. Yang, F. Zhang, *Angew Chem Int Ed Engl.* **2012**, *51*, 9896–9899.
[24] C. Teng, X. Yang, C. Yuan, *Org Lett.* **2009**, *11*, 5542–5545.
[25] T. Daeneke, T-H. Kwon, A. B. Holmes, *Nat Chem.* **2011**, *3*, 211–215.
[26] S de Sousa, C. Olivier, L. Ducasse *ChemSusChem.* **2013**, *6*, 993–996.
[27] X-H. Zhang, Z-S. Wang, Y. Cui, *J. Phys. Chem. C.* **2009**, *113*, 13409–13415.
[28] S. Qu, C. Qin, A. Islam, *Chem Commun (Camb).* **2012**, *48*, 6972–6974.
[29] Z.-S. Wang, N. Koumura, Y. Cui, (no) *Chem. Mater.* **2008**, *20*, 3993–4003.
[30] N. Koumura, Z.-S. Wang, S. Mori, *J. Am. Chem. Soc.* **2006**, *128*, 14256–14257.
[31] G. Bordeau, R. Lartia, G. Metge, *J. Am. Chem. Soc.* **2008**, *130*, 16836–16837.
[32] C. Olivier, F. Sauvage, L. Ducasse, *ChemSusChem,* **2011**, *4*, 731–736
[33] M. J. Frisch, G. W. Trucks, H. B. Schlegel, G. E. Scuseria, M. A. Robb, J. R. Cheeseman, G. Scalmani, V. Barone, B. Mennucci, G. A. Petersson, H. Nakatsuji, M. Caricato, X. Li, H. P. Hratchian, A. F. Izmaylov, J. Bloino, G. Zheng, J. L. Sonnenberg, M. Hada, M. Ehara, K. Toyota, R. Fukuda, J. Hasegawa, M. Ishida, T. Nakajima, Y. Honda, O. Kitao, H. Nakai, T. Vreven, J. A.Montgomery, Jr., J. E. Peralta, F. Ogliaro, M. Bearpark, J. J. Heyd, E. Brothers, K. N. Kudin,V. N. Staroverov,R.Kobayashi, J. Normand, K. Raghavachari, A. Rendell, J. C. Burant, S. S. Iyengar, J. Tomasi, M. Cossi, N. Rega, J. M. Millam, M. Klene, J. E. Knox, J. B. Cross, V. Bakken, C. Adamo, J. Jaramillo, R. Gomperts, R. E. Stratmann, O. Yazyev, A. J. Austin, R. Cammi, C. Pomelli, J. W. Ochterski, R. L. Martin, K. Morokuma, V. G. Zakrzewski, G. A. Voth, P. Salvador, J. J. Dannenberg, S. Dapprich, A. D. Daniels, O. Farkas, J. B. Foresman, J. V. Ortiz, J. Cioslowski, D. J. Fox GAUSSIAN 09. Gaussian, Inc., Wallingford CT.
[34] W. Kohn, L. J. Sham, *Phys. Rev.* **1965**, *140*, A1133–A1138.
[35] J. Klimeš, A. Michaelides, *J. Chem. Phys.* **2012**, *137*, 120901.
[36] C. Lee, W. Yang, R. G. Parr, *Phys. Rev.* **1988**, *B 37*,785–789.
[37] T. Yanai, D. P. Tew, N. C. Handy, *Chem. Phys. Lett.* **2004**, *393*,51–57.
[38] R. Ditchfield, W. J. Hehre, J. A. Pople, *J. Chem. Phys.* **1971**, *54*,724–728.
[39] S. Tretiak, S. Mukamel, *Chem. Rev.* **2002**, *102*, 3171–3212.
[40] E. K. U. Gross, J. F. Dobson, M. Petersilka, *Top. Curr. Chem.* **2005**, *181*, 81–172.
[41] C. A. Guido, P. Cortona, C. Adamo, *J. Chem. Phys.* **2014**, *140*, 104101.
[42] A. D. Becke, *J. Chem. Phys.* **1993**, *98*, 5648–5652.
[43] S. I. Gorelsky, A. B. P. Lever, *J. Organomet. Chem.* **2001**, *635*,187–196.
[44] M. Cossi, V. Barone, *J. Chem. Phys.* **2001**, *115*, 4708–4717.
[45] J. P. Foster, F. Weinhold, *J. Am. Chem. Soc.* **1980**, *102*, 7211–7218.
[46] A. Abbotto, N. Manfredi, C. Marinzi, *Energy Environ. Sci.* **2009**, *2*, 1094.
[47] M. Pastore, E. Mosconi, F. de Angelis *J. Phys. Chem. C* .**2010**, *114*, 7205–7212.
[48] J. C. Croney, M. K. Helms, D. M. Jameson, *Biophys. J.* **2003**, *84*, 4135–4143.
[49] R. A. Marcus, *J. Chem. Phys.* **1965**, *43*, 679–701.
[50] R. A. Marcus, *Angew Chem. Int. Ed. Engl.* **1993**, *32*, 1111–1121.
[51] R. A. Marcus, *J. Chem. Phys.* **1956**, *24*, 966–978.
[52] S. M. Feldt, E. A. Gibson, E. Gabrielsson, *J. Am. Chem. Soc.* **2010**, *132*, 16714–16724.